Europ. J. Agronomy 46 (2013) 42–52

Contents lists available at SciVerse ScienceDirect

European Journal of Agronomy

journal homepage: www.elsevier.com/locate/eja

A red-edge spectral index for remote sensing estimation of green LAI over agroecosystems

J. Delegido*, J. Verrelst, C.M. Meza, J.P. Rivera, L. Alonso, J. Moreno

Department of Earth Physics and Thermodynamics, Image Processing Laboratory, Universidad de Valencia, C/Catedrático Agustín Escardino 9, 46980 Paterna, Valencia, Spain

ARTICLE INFO

Article history:
Received 4 April 2012
Received in revised form
30 November 2012
Accepted 9 December 2012

Keywords:
LAI
NDI
Red-edge
Crops growth monitoring
Remote sensing
Sentinel-2

ABSTRACT

Leaf area index (LAI) is a key biophysical parameter for the monitoring of agroecosystems. Conventional two-band vegetation indices based on red and near-infrared relationships such as the normalized difference vegetation index (NDVI) are well known to suffer from saturation at moderate-to-high LAI values (3–5). To bypass this saturation effect, in this work a robust alternative has been proposed for the estimation of green LAI over a wide variety of crop types. By using data from European Space Agency (ESA) campaigns SPARC 2003 and 2004 (Barrax, Spain) experimental LAI values over 9 different crop types have been collected while at the same time spaceborne imagery have been acquired using the hyperspectral CHRIS (Compact High Resolution Imaging Spectrometer) sensor onboard PROBA (Project for On-Board Autonomy) satellite. This extensive dataset allowed us to evaluate the optimal band combination through spectral indices based on normalized differences. The best linear correlation against the experimental LAI dataset was obtained by combining the 674 nm and 712 nm wavebands. These wavelengths correspond to the maximal chlorophyll absorption and the red-edge position region, respectively, and are known to be sensitive to the physiological status of the plant. Contrary to the NDVI (r^2: 0.68), the red-edge NDI correlated strongly (r^2: 0.82) with LAI without saturating at larger values. The index has been subsequently validated against field data from the 2009 SEN3EXP campaign (Barrax, Spain) that again spanned a wide variety of crop types. A linear relationship over the full LAI range was confirmed and the regression equation was applied to a CHRIS/PROBA image acquired during the same campaign. A LAI map has been derived with an RMSE accuracy of 0.6. It is concluded that the red-edge spectral index is a powerful alternative for LAI estimation and may provide valuable information for precision agriculture, e.g. when applied to high spatial resolution imagery.

1. Introduction

Leaf area index (LAI) is a key variable used by crop physiologists and modellers for estimating foliage cover, as well as monitoring and forecasting crop growth, biomass production and yield (Dorigo et al., 2007; Casa et al., 2012). Green LAI is defined as one-sided area of green leaves per unit ground area and is thus directly related to the growth status of the crop (Scurlock et al., 2001). The spatially explicit quantification of LAI over large areas has become an important aspect in agroecological and climatic studies (Dorigo et al., 2007). At the same time, remotely sensed observations are increasingly being applied at a within-field scale for dedicated agronomical monitoring applications (Gianquinto et al., 2011; Sakamoto et al., 2012). For instance, knowledge of the spatial distribution of LAI and chlorophyll content can assist the farmer towards a more precise distribution of fertilizers (e.g. nitrogen dressings) on the field (Houles et al., 2007; Nguyen and Lee, 2006). Because LAI is functionally linked to the canopy spectral reflectance, its retrieval from optical remote sensing data has prompted many studies using various techniques (Aparicio et al., 2000; Baret and Guyot, 1991; Haboudane et al., 2004). Essentially, these retrieval techniques can be classified into two groups (Le Maire et al., 2008; Zheng and Moskal, 2009): (i) empirical retrieval methods, which typically consist of relating the biophysical parameter of interest against spectral data through linear (e.g. vegetation indices) or nonlinear (e.g. machine learning approaches) algorithmic techniques (Broge and Mortensen, 2002; Glenn et al., 2008; Myneni et al., 1995; Verrelst et al., 2012) and (ii) physically-based retrieval methods, which refers to inversion of radiative transfer models (RTMs) against remote sensing observations (e.g. Gobron et al., 2000; Goel, 1987; Houborg and Boegh, 2008; Jacquemoud et al., 1995). Both approaches have their strengths and weaknesses, which led to the development of many hybrid forms. For instance, machine learning methods (e.g. neural networks) are typically trained by synthetic spectra from RTMs (Hastie et al., 2009; Verger et al., 2008).

* Corresponding author. Tel.: +34 963544068; fax: +34 963543261.
E-mail address: Jesus.Delegido@uv.es (J. Delegido).

1161-0301/$ – see front matter © 2012 Elsevier B.V. All rights reserved.
http://dx.doi.org/10.1016/j.eja.2012.12.001

The advantage of vegetation indices is that they allow obtaining relevant information in a fast and easy way and the underlying mechanisms are well-understood. Most widely known is the Normalized Difference Vegetation Index (NDVI) (Rouse et al., 1973). This successful index from the early days of remote sensing expresses the normalized ratio between the reflected energy in the red chlorophyll absorption region and the reflected energy in the NIR due to scattering of light in the intercellular volume of the leaves mesophyll, and provides an indicator of the 'greenness' of the vegetation, which is in a way related to green LAI and chlorophyll content (Baret and Guyot, 1991; Myneni et al., 1995). Nevertheless, the relationship between NDVI and LAI is exponential, for instance NDVI approaches saturation asymptotically under conditions of moderate-to-high LAI values (e.g. >3–5) (Dorigo et al., 2007; Haboudane et al., 2004).

At the same time, during the last two decades there has been rapid technological progress in the development of imaging spectroscopy or hyperspectral sensors that capture 'images' of reflected solar radiation in a large number of narrow bands (typically between 50 and 250 bands) across the visible and near-infrared region (Nguyen and Lee, 2006; Schaepman et al., 2009). Various imaging spectrometers have been mounted onboard aircrafts for the purpose of precision farming applications (e.g. Delegido et al., 2011a; Lee et al., 2004; Meggio et al., 2010; Oppelt and Mauser, 2004). By analysing such imaging spectrometer data, several experiments have demonstrated that an important spectral region related to LAI is to be found in the red-edge region (Lee et al., 2004; Liu et al., 2004; Wu et al., 2010). This is the region where a sharp change in reflectance between wavelengths 690 and 750 nm takes place, and characterizes the transition from chlorophyll absorption to leaf scattering (Clevers et al., 2002). It has been demonstrated that the shape of the red-edge region is strongly influenced by LAI (Delegido et al., 2008; Herrmann et al., 2011; Lee et al., 2004) principally by the slope of the reflectance curve in this region (Filella and Peñuelas, 1994), while an increase in leaf chlorophyll content causes a shift in the red-edge position towards longer wavelengths (Dash and Curran, 2004; Filella and Peñuelas, 1994; Herrmann et al., 2011; Moran et al., 2004).

The promise and potential of hyperspectral narrowband sensors for a wide array of Earth resource applications has motivated the design and also the launch of spaceborne imaging spectrometers. Until now only experimental imaging spectrometers (e.g. HYPERION, HICO, CHRIS) that detect vegetation biophysical properties at high spatial resolution from space exist, but these kinds of space missions are being planned in near future for routinely monitoring land surfaces (e.g. the German's Enmap mission, NASA's HyspIRI mission). Nevertheless, superspectral resolution sensors (more than 10 and less than 50 bands, i.e. in-between multispectral and hyperspectral resolution) onboard of new generation Earth observation spacecrafts have already incorporated red-edge narrowbands. For instance, the forthcoming Sentinel-2 satellite operated by the European Space Agency (ESA), among others for agroecosystems monitoring applications (Malenovsky et al., 2012), has been configured with new narrowbands, centred at 705 nm and 740 nm. The first Sentinel-2, is envisaged to be launched in 2013 and aims to deliver data taken over all land surfaces at a spatial resolution of 10 m, 20 or 60 m (depending on the used bands) at a high revisiting time (each 5th day under cloud-free conditions) (ESA, 2010). Despite the good performances of narrowband red-edge indices in local field experiments, its robustness in a more generic setting, is still an open issue. It remains to be investigated whether new red-edge narrowbands can deliver more robust estimations than conventional indices such as NDVI when applied over image-wide heterogeneous agroecosystems.

Meanwhile, experimental missions such as ESA's Compact High Resolution Imaging Spectrometer (CHRIS) onboard PROBA (Project for On-Board Autonomy) satellite (Barnsley et al., 2004) can serve as benchmark for the evaluation of new and existing hyperspectral spectral indices on their use for space-based vegetation monitoring application. CHRIS/PROBA was designed as a technology demonstrator and initially intended as a one year mission since its launch in 2001. But both the satellite and the CHRIS sensor continue to function well until now, making this sensor very successful (Verrelst et al., 2010). A constraint for operational use, however, is that CHRIS does not deliver operational data streams but only captures images over requested sites. Nevertheless, by using such images acquired over agricultural areas, it is possible to infer the most relevant bands combination that are related to the parameter of interest (Darvishzadeh et al., 2008; Thenkabail et al., 2000; Verrelst et al., 2012). While these kinds of exercises have already been conducted in a theoretical setting using RTMs (Le Maire et al., 2008), or using ground or airborne hyperspectral data for a specific vegetation type such as pasture (Fava et al., 2009; Mutanga and Skidmore, 2004) or a specific crop type (Casa et al., 2012; Thenkabail et al., 2000), the evaluation of optimized indices has not yet been tested over a multitude of crop types and growth conditions using spaceborne data, which is essential when aiming to use an empirically-optimized index over large datasets of space images. This brings us to the following objectives: (i) to infer the most powerful two-band spectral index from CHRIS data in estimating LAI over a wide range of agricultural crops and growth conditions, (ii) to evaluate this spectral index on its robustness for LAI estimating when applied to an independent dataset, and (iii) to compare this index against other established vegetation indices sensitive to LAI.

2. Methods

A variety of spectral vegetation indices have been developed with the objective of passive estimating biophysical parameters based on remotely sensed spectral radiances (Bannari et al., 2007; He et al., 2006). One of the oldest and most widely used indices is the NDVI, formed from the normalized reflectance values either side of the red-edge, which discriminate between live green and other canopy material. Because of having its origin in broadband sensors, which forms still the majority of the Earth observing satellites, and because of its simplicity, NDVI is one of the most extensively applied vegetation indices related to LAI (Glenn et al., 2008; Turner et al., 1999). Empirical approaches are predominant in delivering accurate estimations at local to landscape scale (Cohen et al., 2003; Weissteiner and Kühbauch, 2005). Studies on various vegetation types, e.g. agroecosystems, grass and shrublands, conifer and broadleaf forests (Chen and Cihlar, 1996; Fassnacht et al., 1994; Friedl et al., 1994; Law and Waring, 1994) have led to the general conclusion that the NDVI has considerable sensitivities to LAI, but merely at relatively low LAI values (Turner et al., 1999). Although the level of saturation is variable and species-dependent (Chen et al., 2002; Hoffmann and Blomberg, 2004), it is generally reached at mid-LAI values around 3–5 (Thenkabail et al., 2000; Turner et al., 1999). This means that NDVI may be a good predictor for only low-to-medium LAIs (González-Sanpedro et al., 2008; Hoffmann and Blomberg, 2004; Yao et al., 2008).

With the advent of hyperspectral imagery, various alternatives to the conventional NDVI have been proposed. For instance, a wide range of narrowband vegetation indices have been developed to bypass saturation effects or minimizing effects of confounding factors such as soil background. Table 1 shows some of the most widely indices used. Most of these indices were initially developed for the study of chlorophyll, except SR and OSAVI, which were proposed to study LAI. TVI was proposed for both chlorophyll and LAI. NDVI and others have subsequently been used to study both parameters (Haboudane et al., 2008). In an attempt to further

Table 1
Vegetation indices used in this study, where R_λ is reflectance at wavelength λ (nm).

Index	Formula	Reference
NDVI	$(R_{800}-R_{670})/(R_{800}+R_{670})$	Rouse et al. (1973)
MCARI	$[(R_{700}-R_{670})-0.2(R_{700}-R_{550})]\,R_{700}/R_{670}$	Daughtry et al. (2000)
TCARI	$3[(R_{700}-R_{670})-0.2(R_{700}-R_{550})R_{700}/R_{670}]$	Haboudane et al. (2002)
MTCI	$[(R_{750}-R_{710})/(R_{710}-R_{680})]$	Dash and Curran (2004)
TCI	$1.2(R_{700}-R_{550})-1.5(R_{670}-R_{550})(R_{700}/R_{670})^{1/2}$	Haboudane et al. (2008)
R-M	$R_{750}/R_{720}-1$	Gitelson et al. (2005)
TVI	$0.5[120(R_{750}-R_{550})-200(R_{670}-R_{550})]$	Broge and Leblanc (2000)
OSAVI	$(R_{800}-R_{670})/(R_{800}+R_{670}+0.16)$	Rondeaux et al. (1996)
PRI	$(R_{550}-R_{531})/(R_{550}+R_{531})$	Gamon et al. (1992)
SR	R_{800}/R_{670}	Jordan (1969)
SR705	R_{750}/R_{705}	Gitelson and Merzlyak (1994)

optimize the sensitivity of these indices, some authors started using these indices together as a new index such as MCARI/OSAVI or TCARI/OSAVI (Daughtry et al., 2000; Haboudane et al., 2008; Meggio et al., 2010).A drawback of these established indices, however, is that the most sensitive bands are not necessarily the ones used to construct the index. An alternative approach therefore is calculating all possible two-band narrowband combinations according to the NDVI formulation, being the Normalized Difference Index (NDI_{a-b}):

$$NDI_{a-b}=\frac{R_b-R_a}{R_b+R_a} \quad (1)$$

where $R_{a,b}$ are the reflectance values in the a and b bands in the visible and near-infrared spectral range. Using this approach, it was demonstrated that the best information is contained in only a few selected bands or indices with the rest becoming redundant (Fava et al., 2009; Ray et al., 2006; Thenkabail et al., 2000). Specifically, some authors have demonstrated that the band combination around 670 and 800 nm, as used by NDVI, not always provides best information about LAI, while other regions appeared to be more successful (Thenkabail et al., 2000; Zhao et al., 2007). Zhao et al. (2007) found that the bands with best linear correlation between LAI and cotton field data were 700–710 and 750–900. Similarly, using CHRIS data over a shrubland, Stagakis et al. (2010) found that a strong linear correlation between NDI_{a-b} and LAI when b is between 580 and 720 nm, and a between 710 and 1003 nm. Overall, while showing superiority over NDVI, these studies also showed that the accuracy of different optimized indices depends on several factors related to the biological characteristics of the plant material, and no single index could be considered superior in general. In this work the NDI_{a-b} formulation was used to evaluate all two-band combinations in the range of 600–1000 nm that lead to optimized linear correlation with LAI using spaceborne hyperspectral data. Evaluation was done by calculating the coefficient of determination (r^2). It should thereby being taken into account that instead of aiming at high accuracies for a specific crop type, efforts were undertaken to seek for an optimized index applicable over a large variety of crops agroecosystem. Finally, the best-evaluated regression equation was validated by an independent dataset and compared against the performance of the established indices of Table 1.

3. Experimental dataset

3.1. SPARC

The experimental data used for the development of an optimized LAI-sensitive index was obtained from the SPARC (Spectra Barrax Campaigns) campaigns which were organized by ESA during the summers of 2003 and 2004. The campaigns were conducted at Barrax, La Mancha region in Spain (coordinates 30°3′N, 2°6′W; 700 m altitude). The test area has a rectangular form and an extent of 5 km × 10 km, and is characterized by a flat morphology and large, uniform land-use units. The region consists of approximately 65% dry land and 35% irrigated agricultural parcels. The climate conditions are typically Mediterranean with a hot and dry summer. The annual rainfall average is about 400 mm. The 2003 campaign was conducted between 12 and 14 July, and the 2004 campaign between 15 and 16 July.

Biophysical parameters were measured on various agricultural parcels in total spanning 9 different crop types (garlic, alfalfa, onion, sunflower, corn, potato, sugar beet, vineyard and wheat) and a large set of ground sampling points were identified (240 elementary sample units (ESU) plots from crops and additional 60 samples from bare soils). ESU refers to a plot size of about 20 m × 20 m. In each ESU, among other parameters, LAI was measured with a digital analyzer (Licor LAI-2000), which works by comparing the intensity of diffuse incident illumination measured at the bottom of the canopy with that arriving at the top (LI-COR technical report) (Welles and Norman, 1991). Each LAI value used in the present study was obtained as a statistical mean of 24 measures (8 data readings × 3 replications) with variable standard errors between 5 and 10% (Fernández et al., 2005). Fig. 1 shows an image of the study area with the 2004 campaign crops. The 2003 campaign was on the same area, though there were also some changes in crop cultivation and measured crop types (Delegido et al., 2008; Moreno et al., 2004).

In parallel with the field measurements, four CHRIS/PROBA images were acquired during the days 12 to 14 July 2003 and 15 and 16 July 2004. CHRIS on board PROBA satellite provides high spatial resolution hyperspectral/multiangular data, acquiring 5 consecutive images from 5 different views (fly-by zenith angles 0°, ±36°, ±55°) over a dedicated site in one single satellite overpass. CHRIS measures over the visible/near-infrared spectra from 400 nm to 1050 nm. It can operate in different modes, thereby compromising between the number of spectral bands and the spatial resolution to keep balanced the signal level and data volume. In particular, CHRIS Mode 1 provides 62 bands (bandwidth ranges between 6 nm and 12 nm) and has a spatial resolution of 34 m at nadir (Barnsley et al., 2004). In the 2003 and 2004 campaigns, the sensor was configured at highest spectral resolution Mode 1, which is most favourable for vegetation studies. The images were first geometrically corrected (Alonso and Moreno, 2005) and then atmospherically corrected according to the method proposed by Guanter et al. (2005). This method simultaneously derives a set of calibration coefficients and an estimation of water vapour content and aerosol optical thickness from the data themselves. The atmospheric correction of the data was validated by direct comparison of CHRIS-derived reflectance retrievals with simultaneous ground-based measurements acquired during the campaigns, as is described in Guanter et al. (2005). From all the angular images acquired during the campaigns, only the ones corresponding to

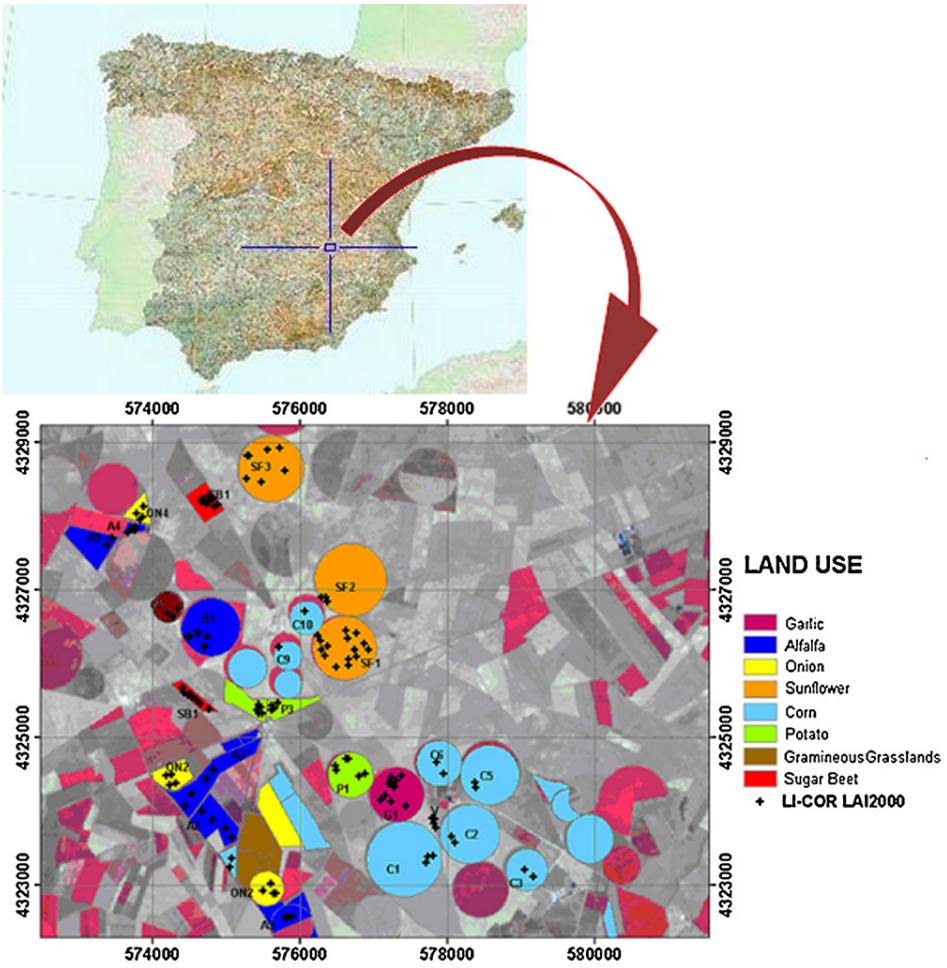

Fig. 1. Land use map, in southeast of Iberian Peninsula, for selected crops during the SPARC 2004 campaign. The points marked with (+) indicate points where LAI was measured. The grid reflects the UTM-projection coordinates (Delegido et al., 2008).

nadir view were selected so that angular and atmospheric effects are minimized, and that highest spatial resolution is preserved.

3.2. SEN3EXP

In view of validating the best performing NDI_{a-b}, an independent dataset was used coming from the SEN3EXP (Sentinel-3 Experiment) campaign. The SEN3EXP campaign was conducted in 2009 and formed part of the European GMES (Global Monitoring for Environment and Security) Sentinel-3 programme (ESA, 2012). The SEN3EXP campaign was set up in a similar way as SPARC; it included collection of field measurements, along with simultaneously acquired hyperspectral observations from various airborne and spaceborne sensors. Several sites across Europe where selected including Barrax as representing a Mediterranean agroecosystem with different water regimes (rainfed and irrigated). The Barrax campaign was carried out during 20–24 June 2009. Similar as in SPARC, elementary sample units (ESUs) were defined wherein LAI and other biophysical parameters were collected.

In this campaign, LAI was measured in 34 ESUs distributed over 14 different agricultural fields (Delegido et al., 2011b) by the methodology of hemispheric photographs, which allows calculating the gap fraction over the angular range of 180° and can be related to LAI (Weiss et al., 2004). LAI measurements were conducted over 9 different crop types, being sunflowers, sugar beet, almond trees, alfalfa, garlic, corn, vineyard, onion and potato, with LAI varying between 0 and 3 for the majority of the crops, and with an LAI around 7 for potatoes. The ESUs are marked by the labels on the agricultural parcels in Fig. 2.

Along with the field measurements, several spaceborne CHRIS Mode 1 images were acquired the 19 and 29 June 2009. In this work we used the 19 June CHRIS image, which is most close to the period of field measurements. The images were geometrically and atmospherically preprocessed according to the same methodology as described in the above-mentioned SPARC campaign.

4. Results

4.1. NDVI

The SPARC field dataset, along with the ensemble of CHRIS images, was used to develop a simple spectral method applicable for remote sensing estimation of LAI over a complete set of different agroecosystems. As a reference, NDVI values were first calculated from the CHRIS reflectance spectra and were subsequently plotted against the corresponding measured LAI values (Fig. 3). Although a linear regression through the scatter plot led to an r^2 of 0.687, note from this figure that NDVI starts saturating already around a LAI of 3. Alternatively, a power function, plotted in Fig. 3, led to a similar r^2 of 0.681 and thus it did not improve the

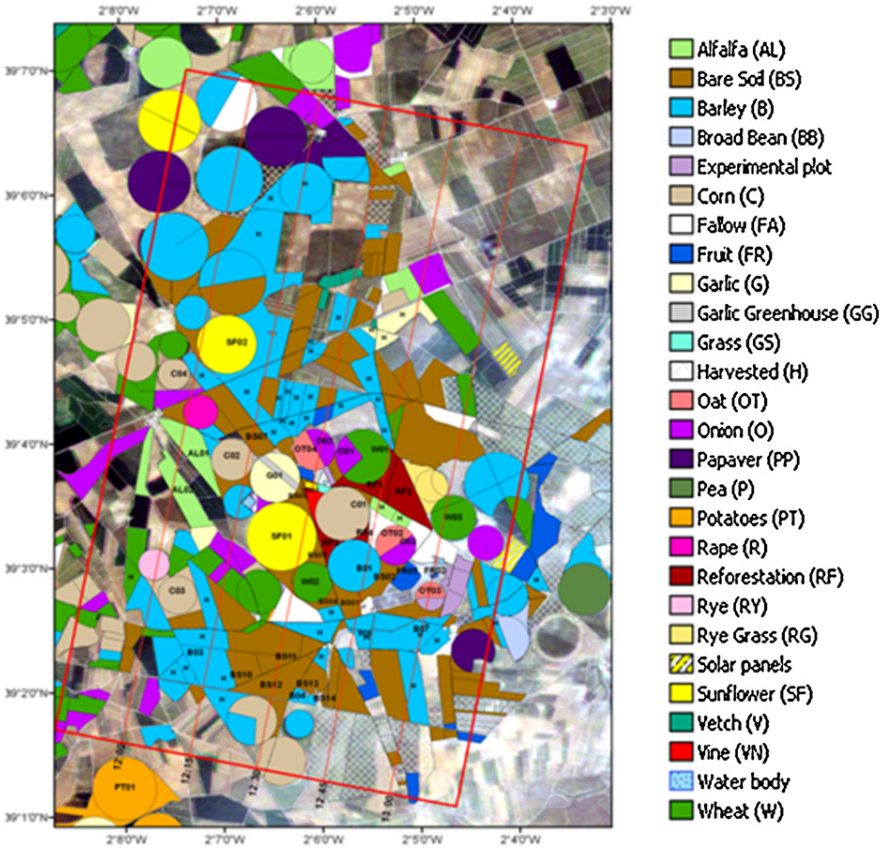

Fig. 2. Land use map of the study area during SEN3EXP campaign. The area in which measurements were made is marked in red (Delegido et al., 2011b). (For interpretation of the references to colour in this figure legend, the reader is referred to the web version of this article.)

relationship. Given that crops can easily reach LAIs of above 4 (e.g. potatoes, corn, sugar beet), this saturation is a major obstacle to the use of NDVI-related relationships for crop monitoring applications.

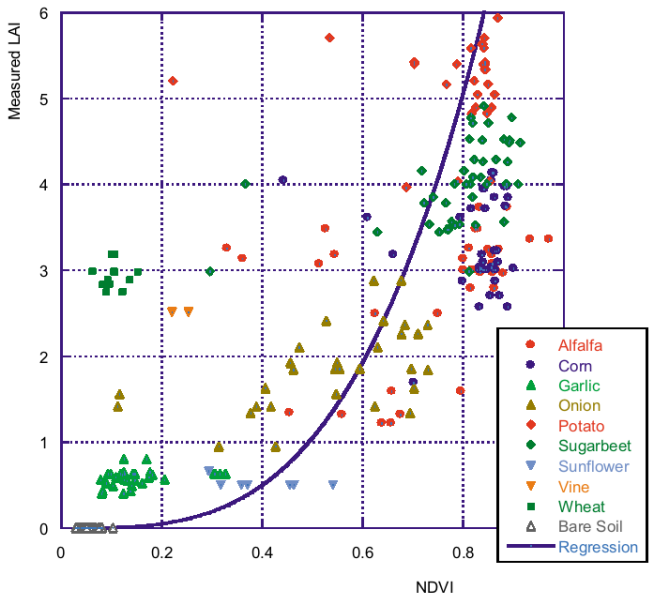

Fig. 3. Measured LAI plotted against NDVI derived from CHRIS spectra (SPARC dataset).

4.2. Generic NDI_{a-b}

To optimize the retrieval of LAI by means of spectral indices, all possible two-band combinations have been calculated from CHRIS spectra in the form of generic NDI_{a-b} (according to Eq. (1)) with a and b in the region from 600 to 1000 nm. Each of these indices was subsequently correlated with green LAI using linear regression and statistics such as the coefficient of determination (r^2) and the p-value were calculated. One of the resulting correlation matrices, shown in Fig. 4a, enables us to inspect variation in the r^2 coefficient over all the two-band combinations. The figure is marked by an optimized region shown in green with strong correlations and a maximum r^2 of 0.717 was obtained by the two-band combination of $a = 674$ and $b = 712$ nm bands. In CHRIS, the 674 nm waveband has a bandwidth of 10 nm while the 712 nm band has bandwidth of 6 nm. With these two spectral bands positioned in the red and in the lower part of the red-edge, highest sensitivity towards variation in green LAI is obtained. Both bands show sensitivity to LAI and chlorophyll variations, and can be considered as the coupling of a chemical absorption (chlorophyll) to a structural variable (LAI). Specifically, 674 nm is located in a relative chlorophyll absorption maximum and 712 nm is located in the red-edge region, where the variability is driven by the transition from a maximum to a minimum of chlorophyll absorption and the slope on the red-edge is directly related to structural effects, in particular LAI (Filella and Peñuelas, 1994). This increases the sensitivity of the index to green LAI and explains the obtained optimized result. In comparison, the conventional NDVI region with $a = 674$ nm and $b = 803$ nm can also be viewed in the same figure. Though it can be noted that this point did not lead to most optimal correlations in the matrix; it performed about 4% poorer compared to the optimized NDI_{a-b}.

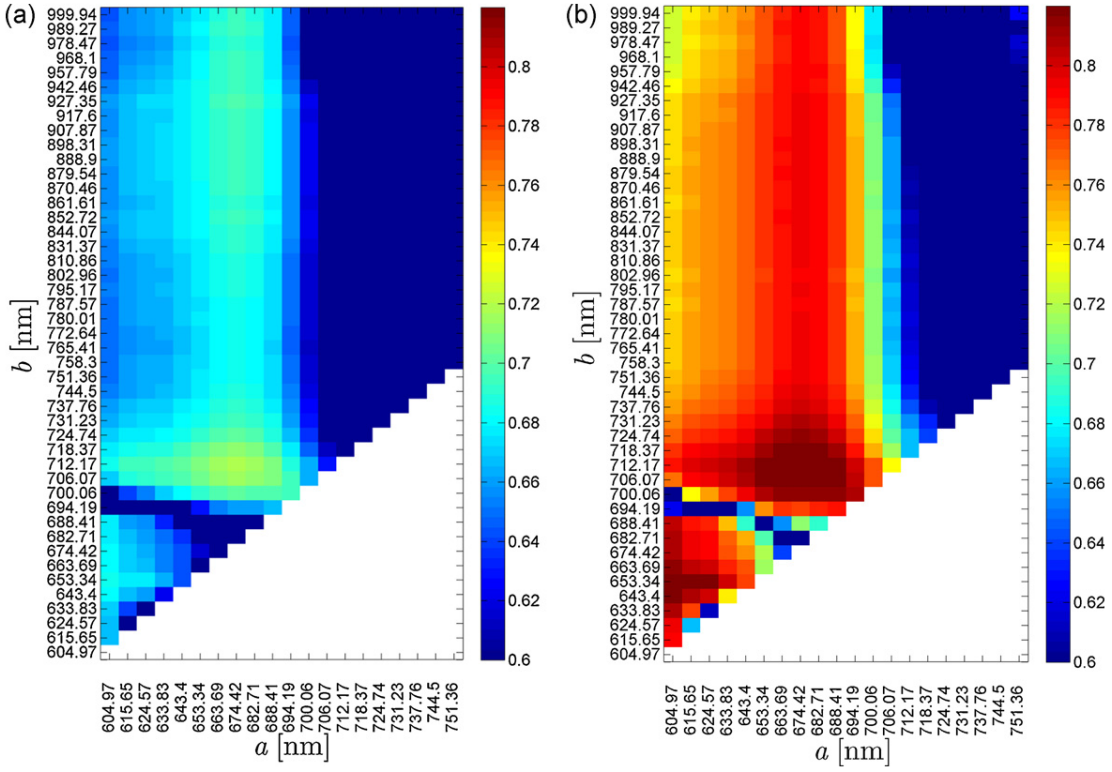

Fig. 4. (a) Linear determination coefficient r^2 between measured LAI and NDI_{a-b} for different combinations of bands a and b (nm). (b) Coefficient r^2 between measured LAI and calculated by NDI_{a-b} for different combinations of bands a and b (nm) without considering the outliers as identified in Fig. 5. Both figures were colour scaled between r^2 of 0.6 and 0.85.

It is also noteworthy that another region of combinations led to optimized results higher up at 674 and 927 nm (in green). In all of these combinations yielded the 674 nm band best performances. With respect to b in the NDI_{a-b} formulation, over the whole matrix the best correlations were obtained precisely within the red-edge region, at 712 nm. Hence, given all possible two-band combinations, an NDI_{a-b} of $a = 674$, which is also used by NDVI, and $b = 712$ nm, which falls right in the red-edge, was found to estimate most accurately green LAI. This optimized NDVI is hereafter referred to as "red-edge NDI" and denoted as $NDI_{674-712}$.

Given the above-identified best performing red-edge NDI, Fig. 5 shows the resulting relationship between its values and the measured LAI values in a scatterplot. A linear relationship can be fitted through the data points according to the following regression equation:

$$LAI = 6.769 NDI_{674-712} \quad r^2 = 0.717 \tag{2}$$

Although a satisfactory relationship was obtained, some sampling points fell away from the linear trend (marked with a circle in Fig. 5). Those 12 points have been identified as belonging to senescent wheat plants, i.e. with dry and yellowish leaves, and thus do not represent green vegetation. Reflectance spectra of senescent vegetation resemble closely to dry soil spectra and cannot be detected by an NDI_{a-b} index that is only sensitive to variations in green leaves. Therefore, those data points have been reasonably removed from the fit, resulting in an improved correlation:

$$LAI = 6.753 NDI_{674-712} \quad r^2 = 0.824 \tag{3}$$

Given the variety of crop types included, this relationship seems to be sufficiently robust for assessing green LAI from spaceborne superspectral or hyperspectral imageries in a simple way.

In order to assess the influence of these discarded data points the r^2 matrix was recalculated without the outliers (Fig. 4b). It can be noted that the correlations improved considerably and the same optimal band combinations clearly emerged.

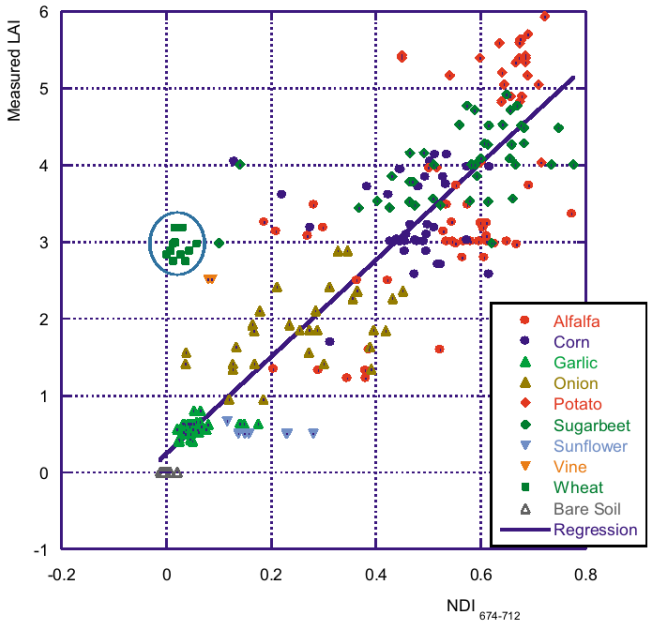

Fig. 5. Measured LAI plotted against NDI_{a-b} derived from CHRIS spectra using wavebands at a: 674 nm and b: 712 nm (SPARC dataset).

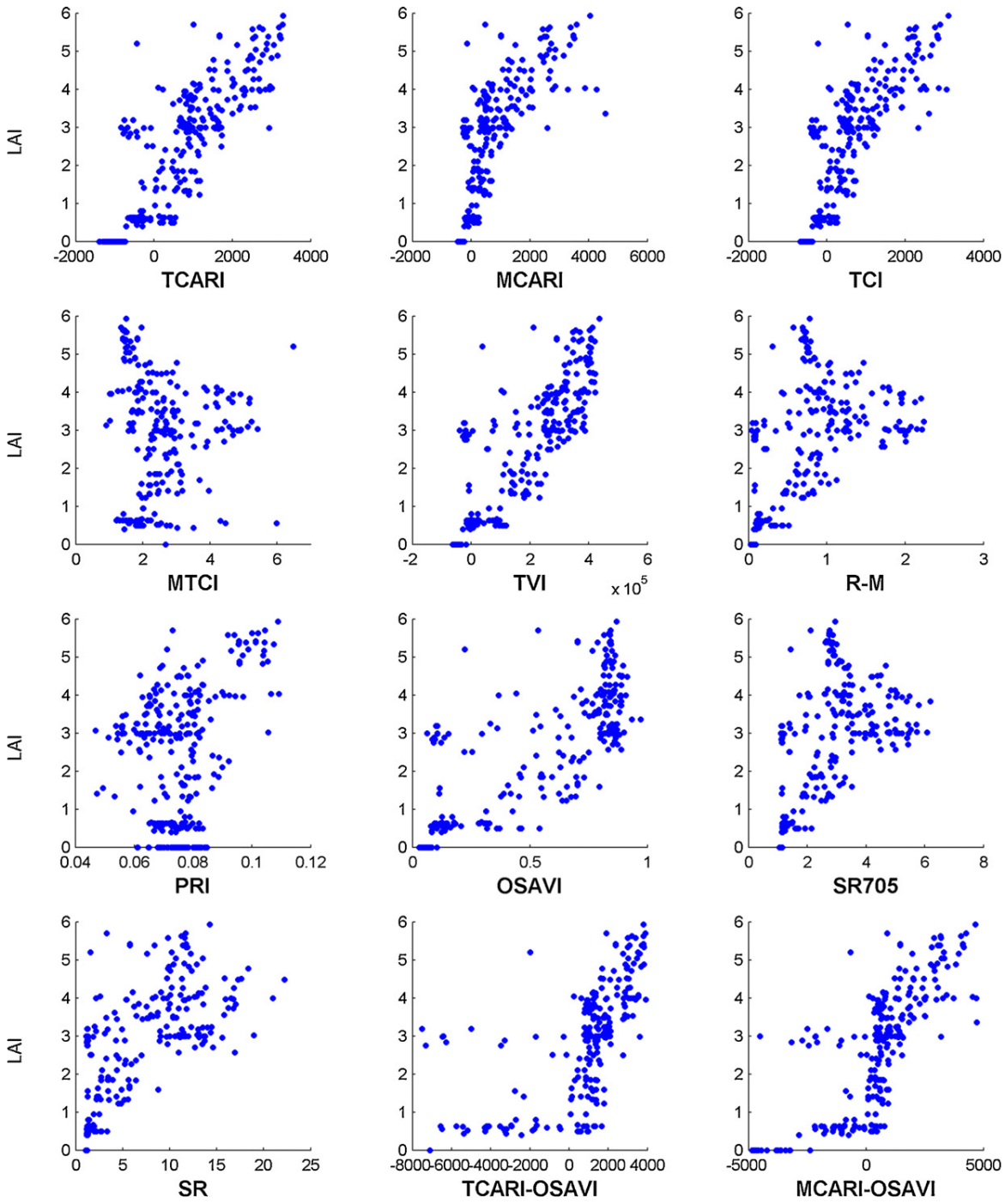

Fig. 6. Measured LAI in SPARC campaigns according to the selected Table 1 indices.

4.3. Comparison with other indices

In comparison, also the performance of established indices has been evaluated. Fig. 6 shows experimental LAI dataset of the SPARC field campaign plotted against the values of the selected indices. Along with these graphs Table 2 shows the corresponding r^2 coefficients and p-values. Overall poorer correlations than the proposed NDI were obtained but two indices showed a slightly better linear relationship with LAI, being TCARI and TVI. Remarkably, both of these indices use three bands instead of two which may

Table 2
r^2 coefficients and p-values for the differents graphs of Fig. 6.

	MCARI	TCARI	MTCI	TCI	R-M	TVI	OSAVI	PRI	SR	SR705	MCARI SAVI	TCARI SAVI
r^2	0.614	0.748	0.037	0.705	0.403	0.751	0.688	0.082	0.412	0.438	0.582	0.482
p	<0.0001	<0.0001	<0.0001	<0.0001	<0.0001	<0.0001	<0.0001	<0.0001	<0.0001	<0.0001	<0.0001	<0.0001

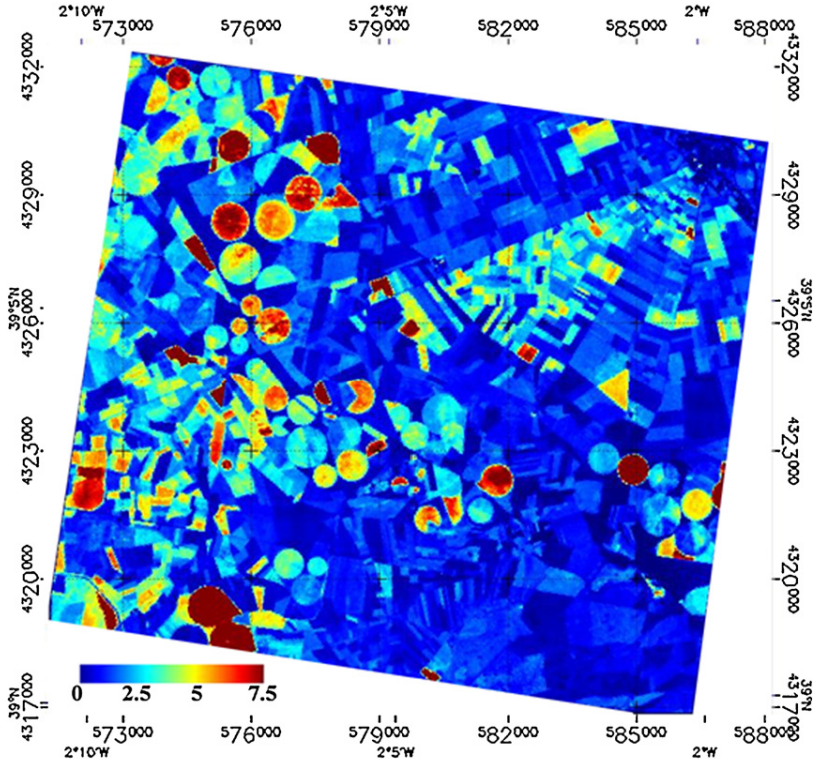

Fig. 7. Final LAI map over the study site as obtained from the 19 June 2009 CHRIS image (SEN3EXP dataset).

explain their good performance. TCARI, TCI and TVI were originally developed for the estimation of chlorophyll content and they are very similar to each other. TCI and TCARI use bands at 550, 670 and 700 nm, while TVI uses 550, 670 and 750 nm. Chlorophyll absorption is maximized at 670 nm whereas a large portion of the solar radiation is reflected at 550 nm. These bands in combination with bands around the red-edge (700, 750 nm) proved to be successful for estimating LAI (see also Lee et al., 2004; Thenkabail et al., 2000; Zhao et al., 2007). The remaining indices yielded poor correlation with LAI, either because not using the 670 nm band or bands in the red-edge region or because of combining indices that caused reduced sensitivity, like MCARI/OSAVI, TCARI/OSAVI, originally used to provide predictive relationships for chlorophyll estimation in precision agriculture (Haboudane et al., 2008; Meggio et al., 2010).

4.4. Validation

Validation of retrieval methods using independent datasets is an important step in evaluating its actual performance. The SEN3EXP dataset was used for validation of the red-edge NDI on its capability in estimating LAI. Similar to the SPARC approach, a CHRIS image was first used. The red-edge NDI was calculated. LAI field measurements were subsequently linked to the corresponding red-edge NDI values. The results can be linearly fitted by a regression line according to the following equation:

$$\mathrm{LAI} = -0.91876 + 13.448\mathrm{NDI}_{672.7-710.5} \quad r^2 = 0.905 \tag{4}$$

where NDI_{a-b} has been calculated using the 672.70 and 710.50 nm bands, as over time CHRIS bands have suffered from a small spectral displacement. The regression equation yielded a strong linear correlation with field LAI measurements. Subsequently the final step consists of applying this equation over the 29 June 2009 CHRIS image, which leads to a LAI map over the Barrax agroecosystems (Fig. 7).

Given the final map in Fig. 7, different agricultural parcels can be distinguished based on spatial patterns of LAI estimations. The dark-blue-to-blue colour tones represent low LAI distributions, ranging from values close to zero to two and cover bare soils and sparsely vegetated crop types (onion and some fields of garlic, sunflowers and corn which are in early growth stage) or row crop types that at pixel-level exhibit a low plant cover such as vineyards. The light-blue-to-yellow colour tones represent LAI values between 2 and 3 and cover the majority of major crop types such alfalfa, garlic and some more developed corn and sunflowers. The dark-red parcels represent potatoes fields with a high LAI around 7. Overall, the map shows that the proposed red-edge NDI performs adequately for obtaining large areas LAI maps over an entire agroecosystem from space-based imagery.

Furthermore, Fig. 7 shows that the methodology applied to high spatial resolution imagery allows identification of within-field variations in LAI, which makes the approach potentially applicable to precision farming.

The validity of the LAI map in Fig. 7 was assessed by calculating the root mean square error (RMSE). To do so, we have plotted the LAI field measurements against the estimates obtained from the map (Fig. 8). It led to an RMSE deviation between measured and estimated LAI of 0.55. Note hereby the extremely high measured LAI vales over potatoe crops observed both in the derived map as in the field.

5. Discussion

Since agro-technical decisions are routinely made by the farmer once or twice a week, a simple, robust and up-to-date monitoring application would be most welcome. Specifically, frequent availability of LAI maps will allow the farmer to better monitor agroecosystems dynamics in time at the landscape level (Dorigo et al., 2007). With the advent of high spatial resolution and superspectral sensors, remote sensing techniques have become

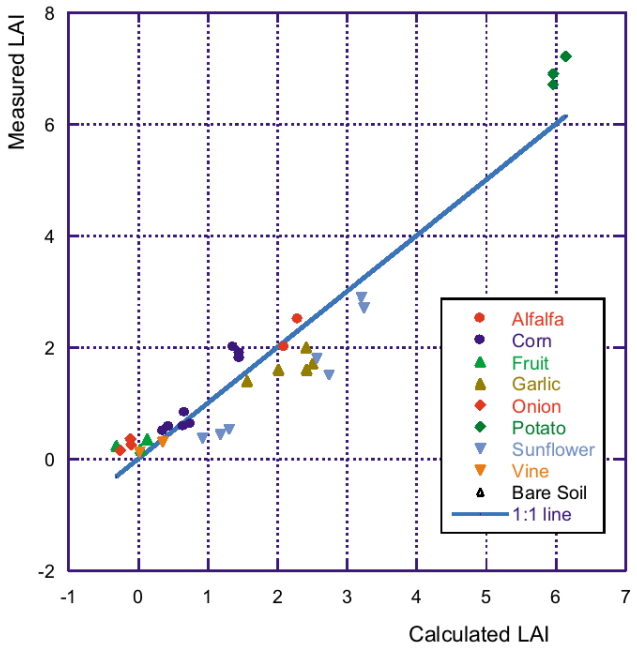

Fig. 8. Measured LAI versus estimated LAI derived from CHRIS spectra using Eq. (4) (SEN3EXP dataset.)

particularly attractive for assessing crop biophysical parameters such as LAI. For instance ESA's forthcoming superspectral Sentinel-2 mission will soon become available to users. Sentinel-2 has a spectral band-settings that is optimized for measuring in red-edge region, and is dedicated to vegetation and agroecosystem monitoring applications at a high spatial (up to 10 m) and temporal resolution. Under cloud-free conditions Sentinel-2 revisit the same site about each 5th day (ESA, 2010), which would allow the farmer to monitor crop growth on a weekly basis. This monitoring could be done through image-wide LAI mapping by applying the here proposed red-edge NDI ($NDI_{674-712}$). It is foreseen that the availability of these kinds of LAI maps will open new agroecosystem monitoring application in the coming years, ranging from field up to global scale (Casa et al., 2012).

The simple regression equation is intended for rapid prediction of LAI in a straightforward way. In fact, regression models based on spectral vegetation indices may be preferable to physically-based models that are complex to design and parameterize (Liang, 2007; Richter et al., 2009). Statistical approaches are amongst the simplest way to predict biophysical parameters, however it does not escape our attention that they provide relationships that are significantly space, time and species dependent (Casa et al., 2012; Glenn et al., 2008; Verrelst et al., 2008). In this respect, it should be stressed that the objective of this article was not the development of a regression equation itself, but rather the delivering of a more robust index that could bypass much of the difficulties experienced with broadband indices. The here proposed red-edge NDI proved to be successful in establishing a linear relationship with green LAI without being prone to saturation at higher LAI values. It should herewith be noted that the observed relationships have been derived purely from experimental data, without involving any modelling that makes assumptions about underlying mechanisms in establishing biochemical/structural relationships. Although regression coefficients can vary depending on the local situation and sensor characteristics, validation of the red-edge NDI proved that the intrinsic relationship between LAI and the index was essentially stable. Henceforth, regression coefficients can be easily recalibrated.

The regression equation was validated against an independent dataset (SEN3EXP). Herewith, it appeared that the linear fitting between NDI and LAI deviated somewhat between model development (SPARC) and validation data. Apart from differences in local conditions, this can also be due to imperfections in the atmospheric correction or due to spectral degradation of the CHRIS sensor. It should be mentioned that CHRIS/PROBA, being an experimental satellite with initially a one year lifetime suffers from a small shifting of wavelengths over time. Bands that were originally configured at 674.42 nm and 712.17 nm were shifted to shorter wavelengths to 672.70 nm and 710.50 nm. While this shift of 2 nm does not impact much the relatively stable red spectral region, it may have considerable impact in the red-edge region. Because of its characteristic steep slope, it means that a 2 nm shift can cause significant changes in the NDI_{a-b}, i.e., being lower positioned in the red-edge slope. Nevertheless, this anomaly is not foreseen to occur when the method is applied to images originating from sensors designed for operational use, such as forthcoming ESA's Sentinel-2 which aims to deliver a consistent data flow for 12 years long (ESA, 2010).

To end with, the red-edge NDI has been compared against established indices. Only the 3-band indices TCARI, TCI and TVI showed good sensitivities to LAI. Both of these indices rely on bands at 550, 670 and around the red-edge region (700, 750 nm), although it remains to be evaluated whether these were the most optimized bands in more variable crop conditions. This suggests that it would be worthwhile to analyze further the use of generic and established more advanced (3- or 4-band) indices and relate them to multiple biophysical parameters such as LAI, chlorophyll content and fractional vegetation cover. On the other hand, it is of importance identifying whether promising indices, e.g. the red-edge NDI, possess a strong universality. Therefore, in a follow-up study we aim to further evaluate the utility of promising indices over different vegetation types and atmospheric conditions, e.g. by using data of other campaigns (Delegido et al., 2011a).

6. Conclusions

While the utility of the red-edge spectral region has been demonstrated in various studies, the majority of these studies have developed empirical relationships with green LAI on the basis of ground or airborne hyperspectral data, typically only for one crop type or in one growth stage. In addition to existing indices, in this work a red-edge normalized difference index (NDI) has been proposed and validated using spaceborne hyperspectral data over a large variety of crops. Based on LAI field measurements and CHRIS hyperspectral data simultaneously collected during the summer 2003 and 2004 ESA SPARC campaigns, we have fully exploited the hyperspectral information available in the CHRIS image. LAI data were collected over 10 different crop types in various phenological states and water regimes. The predictive power of all available two-band combinations have been analyzed according to NDI_{a-b}, a generic variation of the NDVI formulation. The wavebands that led to best correlation with the LAI dataset were encountered at 674 nm, which is precisely situated in the region of maximal chlorophyll absorption and also used by the conventional NDVI, and at 712 nm, which is situated in the red-edge region, a region that is strongly related to the physiological status of the plant (red-edge slope related to LAI). It led to an r^2 of 0.82, and contrary to the NDVI this proposed red-edge NDI did not lead to saturation at higher LAI values. Another two-band region with high correlations has been detected in the waveband situated around 674 (same as red-edge NDI) and 927 nm, situated in the NIR. Such index can be of interest in view of sensors that have no red-edge bands available. The red-edge NDI has been subsequently compared against other widely

used established vegetation indices using the SPARC dataset. The red-edge NDI outperformed most of the indices but also the 3-band indices TCARI, TCI and TVI showed good sensitivities to LAI with an r^2 on the order of 0.75.

Finally, the predictive power of the red-edge NDI has been validated by independent LAI field measurements and satellite observations collected over the same site during the 2009 SEN3EXP campaign. It was observed that a high linear correlation was maintained, although the numerical result depends on the slope of the regression line. The obtained regression equation was applied to a CHRIS image for LAI mapping and validated with an RMSE deviation between measured and estimated LAI of 0.6.

The methodology allows identification of within-field variations in LAI, which makes the approach potentially applicable to precision farming when applied to high spatial resolution imagery.

Acknowledgement

This work has been made possible by the project AYA2010-21432-C02-01, funded by the Spanish Ministry of Economy and Competitiveness. J. Verrelst is supported by the EU Marie Currie IEF grant #252237.

References

Alonso, L., Moreno, J., 2005. Advances and limitations in a parametric geometric correction of CHRIS/Proba data. In: Proceedings of the 3rd CHRIS/Proba Workshop, ESA/ESRIN, Frascati, Italy, Available on line at: http://earth.esa.int/workshops/chris_proba_05/papers/06_alonso.pdf

Aparicio, N., Villegas, D., Casadesus, J., Araus, J.L., Royo, C., 2000. Spectral vegetation indices as nondestructive tools for determining durum wheat yield. Agronomy Journal 92, 83–91.

Bannari, A., Khurshid, K.S., Staenz, K., Schwarz, J.W., 2007. A comparison of hyperspectral chlorophyll indices for wheat crop chlorophyll content estimation using laboratory reflectance measurements. IEEE Transactions on Geoscience and Remote Sensing 45, 3063–3074.

Baret, F., Guyot, G., 1991. Potentials and limits of vegetation indices for LAI and APAR assessment. Remote Sensing of Environment 35, 161–173.

Barnsley, M.J., Settle, J.J., Cutter, M.A., Lobb, D.R., Teston, F., 2004. The PROBA/CHRIS mission, a low-cost smallsat for hyperspectral multiangle observations of the earth surface and atmosphere. IEEE Transactions on Geoscience and Remote Sensing 42, 1512–1520.

Broge, N.H., Mortensen, J.V., 2002. Deriving green crop area index and canopy chlorophyll density of winter wheat from spectral reflectance data. Remote Sensing of Environment 81, 45–57.

Broge, N.H., Leblanc, E., 2000. Comparing prediction power and stability of broadband and hyperspectral vegetation indices for estimation of green leaf area index and canopy chlorophyll density. Remote Sensing of Environment 76, 156–172.

Casa, R., Varella, H., Buis, S., Guérif, M., Solan, B., Baret, F., 2012. Forcing a wheat crop model with LAI data to access agronomic variables. Evaluation of the impact of model and LAI uncertainties and comparison with an empirical approach. European Journal of Agronomy 37, 1–10.

Chen, J.M., Cihlar, J., 1996. Retrieving leaf area index of boreal conifer forests using Landsat TM images. Remote Sensing of Environment 55, 153–162.

Chen, J.M., Pavlic, G., Brown, L., Cihlar, J., Leblanc, S.G., White, H.P., Hall, R.J., Peddle, D.R., King, D.J., Trofymow, J.A., 2002. Derivation and validation of Canada-wide coarse-resolution leaf area index maps using high-resolution satellite imagery and ground measurements. Remote Sensing of Environment 80, 165–184.

Clevers, J.G.P.W., de Jong, S.M., Epema, G.F., van der Meer, F., Bakker, W.H., Skidmore, A.K., Scholte, K.H., 2002. Derivation of the red edge index using MERIS standard band setting. International Journal of Remote Sensing 23, 3169–3184.

Cohen, W.B., Maiersperger, T.K., Gower, S.T., Turner, D.P., 2003. An improved strategy for regression of biophysical variables and Landsat ETM + data. Remote Sensing of Environment 84, 561–571.

Darvishzadeh, R., Skidmore, A., Atzberger, C., Wieren, S., 2008. Estimation of vegetation LAI from hyperspectral reflectance data: effects of soil type and plant architecture. International Journal of Applied Earth Observation 10, 358–373.

Dash, J., Curran, P.J., 2004. The MERIS terrestrial chlorophyll index. International Journal of Remote Sensing 25, 5403–5413.

Daughtry, C.S.T., Walthall, C.K., Kim, M.S., Brown de Costoun, E., McMurtrey, J.E., 2000. Estimating corn leaf chlorophyll concentration from leaf and canopy reflectance. Remote Sensing of Environment 74, 229–239.

Delegido, J., Fernández, G., Gandía, S., Moreno, J., 2008. Retrieval of chlorophyll content and LAI of crops using hyperspectral techniques: application to Proba/CHRIS data. International Journal of Remote Sensing 29, 7107–7127.

Delegido, J., Verrelst, J., Alonso, L., Moreno, J., 2011a. Evaluation of Sentinel-2 red-edge bands for empirical estimation of green LAI and chlorophyll content. Sensors 11, 7063–7081.

Delegido, J., Vergara, C., Verrelst, J., Gandía, S., Moreno, J., 2011b. Remote estimation of crop chlorophyll content by means of high-spectral-resolution reflectance techniques. Agronomy Journal 103, 1834–1842.

Dorigo, W.A., Zurita-Milla, R., de Wit, A.J.W., Brazile, J., Singh, R., Schaepman, M.E., 2007. A review on reflective remote sensing and data assimilation techniques for enhanced agroecosystem modeling. International Journal of Applied Earth Observation 9, 165–193.

ESA, 2010. GMES Sentinel-2 Mission requirements document. http://www.esa.int/esaLP/SEMM4T4KXMF_LPgmes_0.html

ESA, 2012. GMES (Global Monitoring for Environment and Security) info. http://www.gmes.info/

Fassnacht, K.S., Gower, S.T., Norman, J.M., McMurtrie, R.E., 1994. A comparison of optical and direct methods for estimating foliage surface area index in forests. Agricultural and Forest Meteorology 71, 183–207.

Fava, F., Colombo, R., Bocchi, S., Meroni, M., Sitzia, M., Fois, N., Zucca, C., 2009. Identification of hyperspectral vegetation indices for Mediterranean pasture characterization. International Journal of Applied Earth Observation 11, 233–243.

Fernández, G., Moreno, J., Gandía, S., Martínez, B., Vuolo, F., Morales, F., 2005. Statistical variability of field measurements of biophysical parameters in SPARC-2003 and SPARC-2004 campaigns. In: Proc. SPARC Workshop, ESA, Enschede, The Netherlands.

Filella, I., Peñuelas, J., 1994. The red edge position and shape as indicators of plant chlorophyll content biomass and hydric status. International Journal of Remote Sensing 15, 1459–1470.

Friedl, M.A., Michaelsen, J., Davis, F.W., Walker, H., Schimel, D.S., 1994. Estimating grassland biomass and leaf area index using ground and satellite data. International Journal of Remote Sensing 15, 1401–1420.

Gamon, J.A., Peñuelas, J., Field, C.B., 1992. A narrow-waveband spectral index that tracks diurnal changes in photosynthetic efficiency. Remote Sensing of Environment 41, 35–44.

Gianquinto, G., Orsini, F., Fecondini, M., Mezzetti, M., Sambo, P., Bona, S., 2011. A methodological approach for defining spectral indices for assessing tomato nitrogen status and yield. European Journal Agronomy 35, 135–143.

Gitelson, A., Merzlyak, M., 1994. Quantitative estimation of chlorophyll-a using reflectance spectra: experiments with autumn chestnut and maple leaves. Journal of Photochemistry and Photobiology B: Biology 22, 247–252.

Gitelson, A., Viña, A., Ciganda, V., Rundquist, D., Arkebauer, J., 2005. Remote estimation of canopy chlorophyll content in crops. Geophysical Research Letters 32, L08403, http://dx.doi.org/10.1029/2005GL022688.

Glenn, E.P., Huete, A.R., Nagler, P.L., Nelson, S.G., 2008. Relationship between remotely-sensed vegetation indices, canopy attributes and plant physiological processes: what vegetation indices can and cannot tell us about the landscape. Sensors 8, 2136–2160.

Gobron, N., Pinty, B., Verstraete, M.M., Widlowski, J.L., 2000. Advanced vegetation indices optimized for up-coming sensors: design performance and applications. IEEE Transactions on Geoscience and Remote Sensing 38, 2489–2505.

Goel, N.S., 1987. Models of vegetation canopy reflectance and their use in the estimation of biophysical parameters from reflectance data. Remote Sensing Reviews 3, 1–212.

González-Sanpedro, M.C., Le Toan, T., Moreno, J., Kergoat, L., Rubio, E., 2008. Seasonal variations of leaf area index of agricultural fields retrieved from Landsat data. Remote Sensing of Environment 112, 810–824.

Guanter, L., Alonso, L., Moreno, J., 2005. A method for the surface reflectance retrieval from Proba/CHRIS data over land: application to ESA SPARC campaigns. IEEE Transactions on Geoscience and Remote Sensing 43, 2908–2917.

Haboudane, D., Miller, J.R., Tremblay, N., Zarco-Tejada, P.J., Dextraze, L., 2002. Integrated narrow-band vegetation indices for prediction of crop chlorophyll content for application to precision agriculture. Remote Sensing of Environment 81, 416–426.

Haboudane, D., Miller, J.R., Pattey, E., Zarco-Tejada, P.J., Strachan, I.S., 2004. Hyperspectral vegetation indices and novel algorithms for predicting green LAI of crop canopies: modeling and validation in the context of precision agriculture. Remote Sensing of Environment 90, 337–352.

Haboudane, D., Tremblay, N., Miller, J.R., Vigneault, P., 2008. Remote estimation of crop chlorophyll content using spectral indices derived from hyperspectral data. IEEE Transactions on Geoscience and Remote Sensing 46, 423–437.

Hastie, T., Tibshirani, R., Friedman, J.H., 2009. The Elements of Statistical Learning: Data Mining, Inference, and Prediction, second ed. Springer-Verlag, New York.

He, Y., Guo, X., Wilmshurst, J., 2006. Studying mixed grassland ecosystems I: suitable hyperspectral vegetation indices. Canadian Journal of Remote Sensing 32, 98–107.

Herrmann, I., Pimstein, A., Karnieli, A., Cohen, Y., Alchanatis, V., Bonfil, D.J., 2011. LAI assessment of wheat and potato crops by VENμS and Sentinel-2 bands. Remote Sensing of Environment 115, 2141–2151.

Hoffmann, C.M., Blomberg, M., 2004. Estimation of leaf area index of *Beta vulgaris* L. Based on optical remote sensing data. Journal of Agronomy and Crop Science 190, 197–204.

Houborg, R., Boegh, E., 2008. Mapping leaf chlorophyll and leaf area index using inverse and forward canopy reflectance modeling and SPOT reflectance data. Remote Sensing of Environment 112, 186–202.

Houles, V., Guerif, M., Mary, B., 2007. Elaboration of a nitrogen nutrition indicator for winter wheat based on leaf area index and chlorophyll content for making nitrogen recommendations. European Journal of Agronomy 27, 1–11.

Jacquemoud, S., Baret, F., Andrieu, B., Danson, F.M., Jaggard, K., 1995. Extraction of vegetation biophysical parameters by inversion of the PROSPECT + SAIL model

on sugar beet canopy reflectance data – application to TM data. Remote Sensing of Environment 52, 163–172.
Jordan Carl, F., 1969. Derivation of leaf-area index from quality of light on the forest floor. Ecology 50, 663–666.
Law, B.E., Waring, R.H., 1994. Remote sensing of leaf area index and radiation intercepted by understory vegetation. Journal of Applied Ecology 4, 272–279.
Lee, K.S., Cohen, W.B., Kennedy, R.E., Maiersperger, T.K., Gowerd, S.T., 2004. Hyperspectral versus multispectral data for estimating leaf area index in four different biomes. Remote Sensing of Environment 91, 508–520.
Le Maire, G., François, C., Soudani, K., Berveiller, D., Pontailler, S., Bréda, N., Genet, H., Davi, H., Dufrêne, E., 2008. Calibration and validation of hyperspectral indices for the estimation of broadleaved forest leaf chlorophyll content leaf mass per area, leaf area index and leaf canopy biomass. Remote Sensing of Environment 112, 3846–3864.
Liang, S., 2007. Recent developments in estimating land surface biogeophysical variables from optical remote sensing. Progress in Physical Geography 31, 501–516.
Liu, J., Miller, J.R., Haboudane, D., Pattey, E., 2004. Exploring the relationship between red edge parameters and crop variables for precision agriculture. In: Geoscience and Remote Sensing Symposium, 2004. IGARSS '04. Proceedings. IEEE International.
Malenovsky, Z., Rott, H., Cihlar, J., Schaepman, M., Garcia-Santos, G., Fernandes, R., Berger, M., 2012. Sentinels for Science: potential of Sentinel-1, -2, and -3 missions for scientific observations of ocean, cryosphere, and land. Remote Sensing of Environment 120, 91–101.
Meggio, F., Zarco-Tejada, P.J., Núñez, L.C., Sepulcre-Cantó, G., González, M.R., Martín, P., 2010. Grape quality assessment in vineyards affected by iron deficiency chlorosis using narrow-band physiological remote sensing indices. Remote Sensing of Environment 114, 1968–1986.
Moran, M.S., Maas, S.J., Vanderbilt, V.C., Barnes, M., Miller, S.N., Clarke, T.R., 2004. Application of image-based remote sensing to irrigated agriculture. In: Ustin, S.L. (Ed.), Remote Sensing for Natural Resource Management and Environmental Monitoring, Manual of Remote Sensing. John Wiley & sons, Hoboken, pp. 617–676.
Moreno, J., Alonso, L., Fernández, G., Fortea, J.C., Gandía, S., Guanter, L., García, J.C., Martí, J.M., 2004. The spectra Barrax campaing (SPARC): overview and first results from Chris data. In: Proceedings of the 2nd CHRIS/Proba Workshop, ESA/ESRIN, Frascati, Italy, Available online at http://earth.esa.int/workshops/chris_proba_04/papers/10_MOREN.pdf
Mutanga, O., Skidmore, A.K., 2004. Hyperspectral band depth analysis for a better estimation of grass biomass (*Cenchrus ciliaris*) measured under controlled laboratory conditions. International Journal of Applied Earth Observation 5, 87–96.
Myneni, R.B., Maggion, S., Iaquinta, J., Privette, J.L., et al., 1995. Optical remote sensing of vegetation: modeling, caveats, and algorithms. Remote Sensing of Environment 51, 169–188.
Nguyen, H.T., Lee, B.-W., 2006. Assessment of rice leaf growth and nitrogen status by hyperspectral canopy reflectance and partial least square regression. European Journal of Agronomy 24, 349–356.
Oppelt, N., Mauser, W., 2004. Hyperspectral monitoring of physiological parameters of wheat during a vegetation period using AVIS data. International Journal of Remote Sensing 25, 145–159.
Ray, D., Das, G., Singh, J.P., Panigrahy, S., 2006. Evaluation of hyperspectral indices for LAI estimation and discrimination of potato crop under different irrigation treatments. International Journal of Remote Sensing 27, 5373–5387.
Richter, K., Atzberger, C., Vuolo, F., Weihs, P., D'Urso, G., 2009. Experimental assessment to the Sentinel-2 band setting for RTM-based LAI retrieval of sugar beet and maize. Canadian Journal of Remote Sensing 35, 230–247.
Rondeaux, G., Steven, M., Baret, F., 1996. Optimization of soil-adjusted vegetation indices. Remote Sensing of Environment 55, 95–1907.
Rouse, J.W., Haas, R.H., Schell, J.A., Deering, D.W., 1973. Monitoring vegetation systems in the great plains with ERTS. In: Third ERTS Symposium, NASA SP-351, vol. 1, NASA, Washington, DC, pp. 309–317.
Sakamoto, T., Gitelson, A., Nguy-Robertson, A., Arkebauer, T., Wardlow, B., Suyker, A., Verma, S., Shibayama, M., 2012. An alternative method using digital cameras for continuous monitoring of crop status. Agricultural and Forest Meteorology 154, 113–126.
Schaepman, M.E., Ustin, S.L., Plaza, A.J., Painter, T.H., Verrelst, J., Liang, S., 2009. Earth system science related imaging spectroscopy—an assessment. Remote Sensing of Environment 113, 123–137.
Scurlock, J.M.O., Asner, G.P., Gower, S.T., 2001. Worldwide historical estimates and bibliography of leaf area index, 1932–2000. In: ORNL Technical Memorandum TM-2001/268, Oak Ridge National Laboratory, Oak Ridge, Tennessee, U.S.A.
Stagakis, S., Markos, N., Sykioti, O., Kyparissis, A., 2010. Monitoring canopy biophysical and biochemical parameters in ecosystem scale using satellite hyperspectral imagery: an application on a *Phlomis fruticosa* Mediterranean ecosystem using multiangular CHRIS/PROBA observations. Remote Sensing of Environment 114, 977–994.
Thenkabail, P., Smith, R.B., Pauw, E., 2000. Hyperspectral vegetation indices and their relationships with agricultural crop characteristics. Remote Sensing of Environment 71, 158–182.
Turner, D.P., Cohen, W.B., Kennedy, R.E., Fassnacht, K.S., Briggs, J.M., 1999. Relationships between leaf area index and Landsat TM spectral vegetation indices across three temperate zone sites. Remote Sensing of Environment 70, 52–68.
Verger, A., Baret, F., Weiss, M., 2008. Performances of neural networks for deriving LAI estimates from existing CYCLOPES and MODIS products. Remote Sensing of Environment 112, 2789–2803.
Verrelst, J., Schaepman, M.E., Koetz, B., Kneubuhler, M., 2008. Angular sensitivity analysis of vegetation indices derived from CHRIS/PROBA data. Remote Sensing of Environment 112, 2341–2353.
Verrelst, J., Clevers, J.G.P.W., Schaepman, M.E., 2010. Merging the Minnaert-k parameter with spectral unmixing to map forest heterogeneity with CHRIS/PROBA data. IEEE Transactions on Geoscience and Remote Sensing 48, 4014–4022.
Verrelst, J., Muñoz, J., Alonso, L., Delegido, J., Rivera, J.P., Camps-Valls, G., Moreno, J., 2012. Machine learning regression algorithms for biophysical parameter retrieval: opportunities for Sentinel-2 and -3. Remote Sensing of Environment 118, 127–139.
Weiss, M., Baret, F., Smith, G.J., Jonckheere, I., Coppin, P., 2004. Review of methods for in situ leaf area index (LAI) determination. Part II. Estimation of LAI, errors and sampling. Agricultural and Forest Meteorology 121, 37–53.
Weissteiner, C.J., Kühbauch, W., 2005. Regional yield forecasts of malting barley (*Hordeum vulgare* L) by NOAA-AVHRR remote sensing data and ancillary data. Journal of Agronomy and Crop Science 191, 308–320.
Welles, J.M., Norman, J.M., 1991. Instrument for indirect measurement of canopy architecture. Agronomy Journal 83, 818–825.
Wu, C., Han, X., Niu, Z., Dong, J., 2010. An evaluation of EO-1 hyperspectral Hyperion data for chlorophyll content and leaf area index estimation. International Journal of Remote Sensing 31, 1079–1086.
Yao, Y., Liu, Q., Liu, Q., Li, X., 2008. LAI retrieval and uncertainty evaluations for typical row-planted crops at different growth stages. Remote Sensing of Environment 112, 94–106.
Zhao, D., Huang, L., Li, J., Qi, J., 2007. A comparative analysis of broadband and narrow-band derived vegetation indices in predicting LAI and CCD of a cotton canopy. ISPRS Journal of Photogrammetry 62, 25–33.
Zheng, G., Moskal, L.M., 2009. Retrieving leaf area index (LAI) using remote sensing: theories, methods and sensors. Sensors 9, 2719–2745.